Supporting Information

Supporting Information

Metal-induced microporous aminosilica creates a highly permeable gas-separation membrane

Ufafa Anggarini, Liang Yu, Hiroki Nagasawa, Masakoto Kanezashi and Toshinori Tsuru,*[a]

[a.]Department of Chemical Engineering, Hiroshima University, 1-4-1 Kagamiyama, Higashi-Hiroshima, Hiroshima 739-8527, Japan

Supporting Information

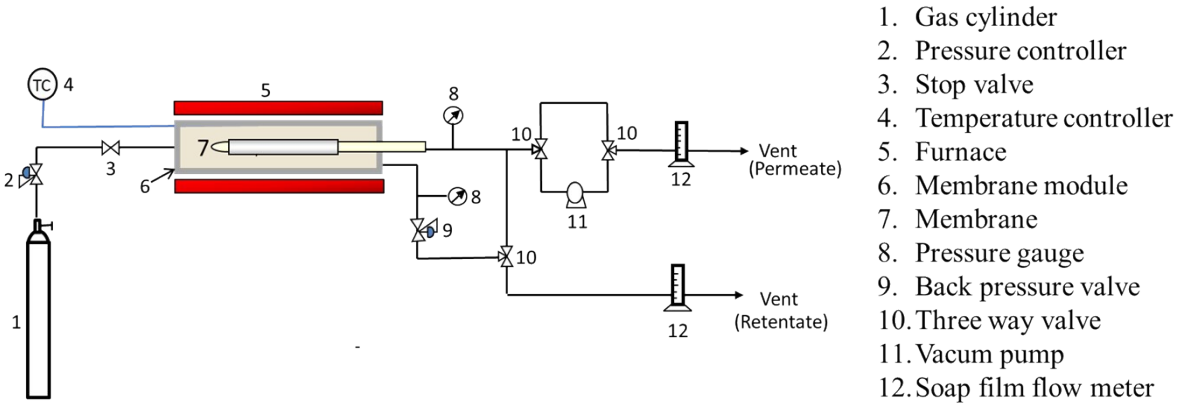

1. Gas cylinder
2. Pressure controller
3. Stop valve
4. Temperature controller
5. Furnace
6. Membrane module
7. Membrane
8. Pressure gauge
9. Back pressure valve
10. Three way valve
11. Vacum pump
12. Soap film flow meter

Fig. S1. Set-up single gas permeation equipment

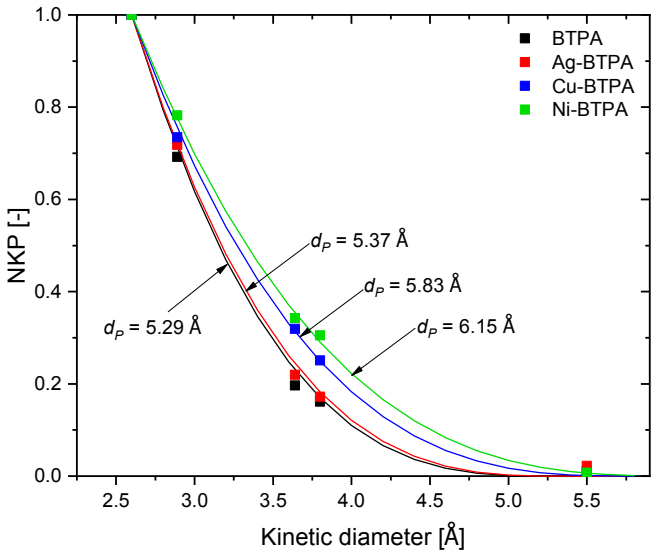

Fig. S2. Pore size prediction based on the NKP method of BTPA and metal-doped BTPA with different metals at 200 °C

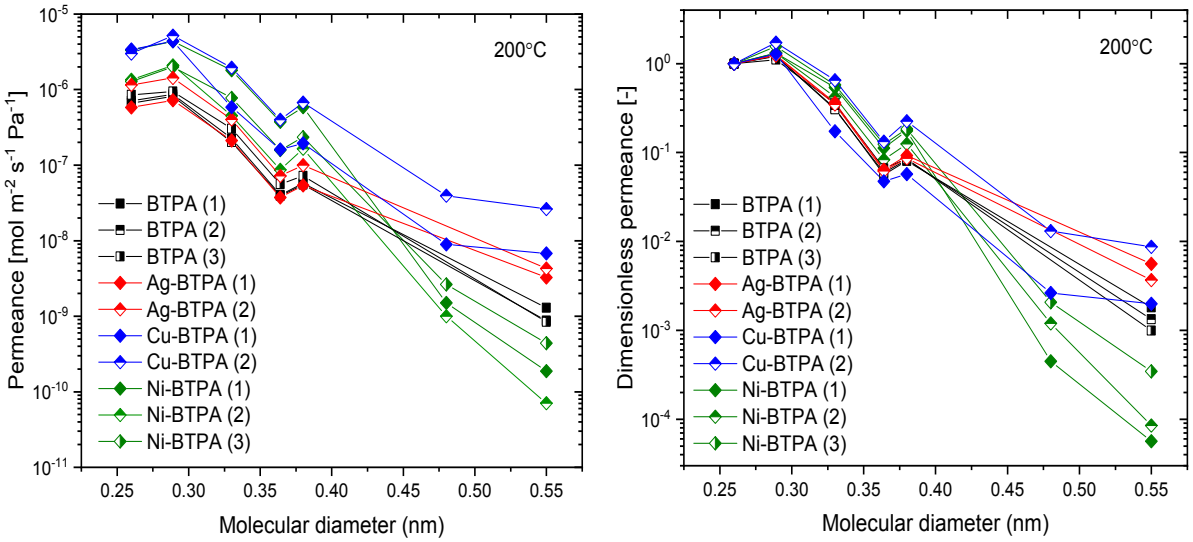

Fig. S3. Reproducible data of single gas permeance for Ni-BTPA as a function of kinetic diameter size of gases measured at 200 °C

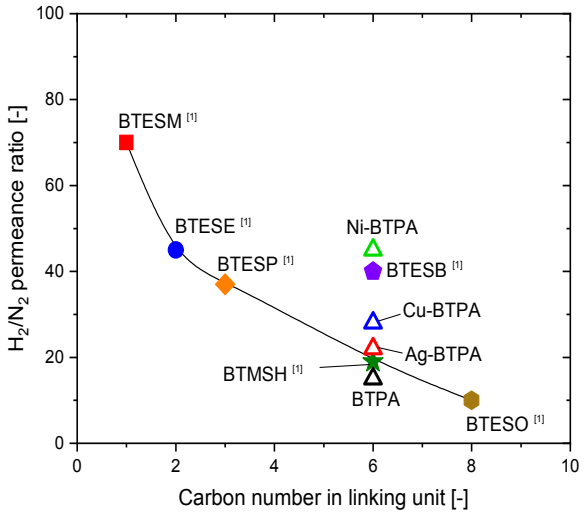

Fig. S4. permeance ratio of H_2/N_2 as a function of carbon number in linking unit of bi-silyl structure

Fig. S4. reveals that there has been a gradual decrease in the H_2/N_2 permeance ratio by increasing the number of carbon molecules between the bi-silyl bridges that gives rise to a higher flexibility in the linking unit [1]. BTPA has a structure that is similar to that of BTMSH (six carbon atoms in linking unit) and shows a H_2/N_2 permeance ratio of 15, which corresponds to the small pore size of the membranes. By contrast, after the addition of metal doping into the BTPA structure, a higher permeance ratio was achieved, which equates to an increase in membrane connectivity and in the rigidity of the linking unit via amine-metal interactions. The linking unit structure transforms from flexible into rigid with increases in the metal affinity.

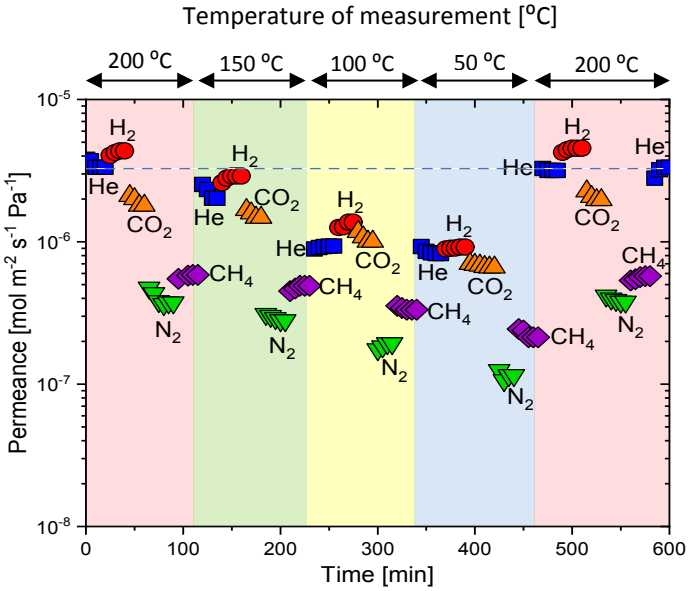

Fig. S5. Effective time courses for Ni-BTPA single-gas permeation performance at different operation temperature (200 °C ⟶ 150 °C ⟶ 100 °C ⟶ 50 °C ⟶ 200 °C)

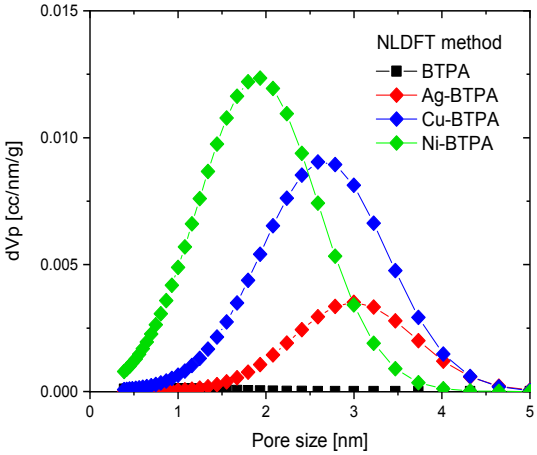

Fig. S6 NLDFT pore size distribution of amorphous aminosilica and metal-doped powder

According to the pore size distribution data in Fig. S6, as affinity for the metal-dopant increased, the pore size distribution narrowed as evident by a decrease in the full width at half maximum (FWHM) value in the NLDFT curve when fitted with a Gaussian function. In this case, the Ni-BTPA showed the most uniform pore size distribution while the BTPA and Ag-BTPA with highly maintained flexible amorphous material showed typically negligible and broad pore size distributions, respectively.

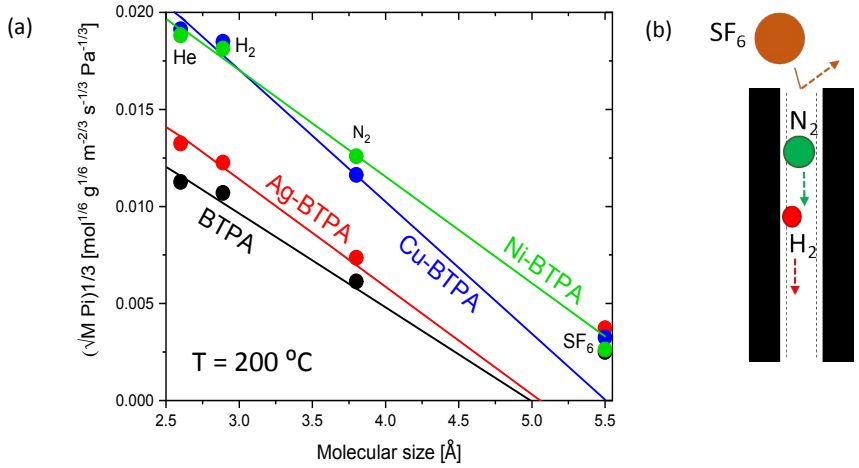

Fig. S7 The correlation of $\left(\sqrt{M_i}P_i\right)^{1/3}$ as a function of molecular size of permeating gases (points and lines are experimental and theoritically calculated, respectively) (a), and schematic gas transport for different gases in a cylindrical pore of Ni-BTPA (b).

The pore size of metal-doped BTPA-derived membranes was estimated by using modified-GT models, as shown in Eq. (1), where the functions of $\left(\sqrt{M_i}P_i\right)^{1/3}$ for different permeating gases were plotted as the sizes of the permeating gases (d_i). As shown in Fig. S7(a), experimental permeation reveals that the membrane pore size was enlarged on the order of Ni-BTPA (6.10 nm) > Cu-BTPA (5.51 nm) > Ag-BTPA (5.06 nm) > BTPA (4.89 nm). Fig. S7(b) presents a schematic illustration of gas transport within cylindrically shaped pores of Ni-BTPA. H_2 and N_2 were accepted within the Ni-BTPA pores, whereas a large gas such as SF_6 was rejected by the repulsive forces between neighboring membrane pore walls. H_2 as a smaller molecule tends to perform at a higher level of potential energy compared with that of N_2. On this occasion, the micropore diffusion rate was determined by the slower passage rate of N_2 through the membrane pore wall [5]. As reported for most microporous organosilica membranes, the gas separation factor is typically at a moderate level for H_2/N_2 separation with a relatively high rate of permeation that relates to a thin topmost layer [5-7]. More importantly, the $\left(\sqrt{M_i}P_i\right)^{1/3}$ of most gases has been the best fit for Ni-BTPA membranes, which indicate that Ni-BTPA consist of uniform pores. On the other hand, other metal-doped BTPA showed points that deviated from the calculated lines, which indicated that the pore sizes were not uniform.

$$\left(\sqrt{M_i}P_i\right)^{1/3} = \left(\frac{k_0}{\sqrt{RT}}exp\left(-\frac{E_{p,i}}{RT}\right)\right)^{1/3}(d_0 - d_i) \quad (1)$$

Supporting Information

Table S1. Summary of He/N_2 and He/SF_6 permeance ratio at 200 °C for different types of organosilica membranes

Membrane material	He/N_2 [-]	He/SF_6 [-]	Ref.
BTESE 6	5.62	1660	[5]
BTESE 6	4.83	133	
BTESE 6	4.14	431	
BTESE 6	5.05	256	
BTESE 60	8.31	4710	
BTESE 60	6.43	7190	
BTESE 60	7.63	220	
BTESE 90	12.5	6310	
BTESE 90	6.99	155	
BTESE 120	25.5	9810	
BTESE 120	21.2	129	
BTESE 120	55.6	296	
BTESE 120	46.3	218	
BTESE 120	30.4	344	
BTESE 120	32.5	632	
BTESE 120	33.1	4170	
BTESE 120	12.2	351	
BTESE 120	15.2	1000	
BTESE 120	11.9	4250	
BTESE 120	18.2	5600	
BTESE 120	25.9	9170	
BTESE 120	7.25	14300	
BTESE 120	10.2	42900	
BTESE 120	45.6	33500	
BTESE 120	21.8	865	
BTESE 120	25	14200	
BTESE 240	39.7	9350	
BTESE 240	28.4	40600	
BTESB	88	2600	[6]
BTESA	10	3300	[7]
BTPA	12	553	This work
BTPA	12	753	
BTPA	12	1010	
Ag-BTPA	11	178	
Ag-BTPA	12	272	
Cu-BTPA	17	502	
Cu-BTPA	4	115	
Ni-BTPA	9	17694	
Ni-BTPA	8	19148	

Ni-BTPA	5	2901

Table S2. Permeation data from different types of membranes for H_2/N_2 separation reported in the reference

Membrane type	Membrane material	H_2 permeance [mol m^{-2} s^{-1} Pa^{-1}]	$\frac{P_{H_2}}{P_{N_2}}$ [-]	Ref.
Aminosilica membranes	BTPA	8.63×10^{-7}	15	This work
	BTPA	9.41×10^{-7}	13	
	BTPA	8.10×10^{-7}	14	
	Ag-BTPA	1.43×10^{-6}	20	
	Ag-BTPA	1.10×10^{-6}	16	
	Cu-BTPA	4.36×10^{-6}	27	
	Cu-BTPA	8.63×10^{-7}	21	
	Cu-BTPA	4.45×10^{-6}	12	
	Ni-BTPA	2.10×10^{-6}	24	
	Ni-BTPA	2.01×10^{-6}	13	
	Ni-BTPA	4.45×10^{-6}	13	
Silica membranes (sol-gel)	TEOS (Tetraethylorthosilicate)	1.00×10^{-7}	31	[8]
	Co-TEOS	4.00×10^{-6}	730	[9]
	Fe/Co-TEOS	8.00×10^{-8}	11	[10]
	BTESE (1,2-bis(triethoxysily)ethane)	1.00×10^{-5}	20	[11]
	Zr-BTESE	1.80×10^{-7}	100	[12]
	TEOS	5.00×10^{-6}	300	[13]
	Ni-TEOS	6.30×10^{-8}	502	[14]
	Ni-TEOS	2.05×10^{-7}	400	[15]
	PCS (polycarbosilane) non-crosslinked	1.00×10^{-9}	190	[16]
		6.00×10^{-9}	20	
	C-PCS (crosslinked polycarbosilane)	1.00×10^{-9}	150	
	PCS oxidized	3.00×10^{-9}	90	
		5.00×10^{-9}	800	
		8.00×10^{-9}	200	
	PS-dispersed PCS	2.00×10^{-8}	200	
		3.00×10^{-8}	100	
Silica membranes (CVD)	TMOS (Tetramethoxysilane)	8.50×10^{-8}	1200	[17]
	Zr-TEOS	7.30×10^{-8}	25	[18]
Porous silica based membranes	BTESA	2.68×10^{-6}	10	[7]
	BTESE	9.50×10^{-7}	22	[19]
	BTESE-400 °C - 0.5 °C - 180min	2.90×10^{-7}	32	[20]
	BTESE-600 °C - 0.5 °C - 180min	1.62×10^{-8}	4	
	BTESE-600 °C - 10 °C - 180min	1.70×10^{-8}	9	
	BTESE-600 °C - 0.5 °C - 5min	4.61×10^{-8}	15	
	BTESEthy	1.27×10^{-7}	22	[7]
	BTESA	3.20×10^{-6}	12	[6]
	BTESAB	2.68×10^{-6}	10	[6]
	TEOS	2.00×10^{-6}	70	[9]
	TEOS	7.00×10^{-9}	23	[21]
	TEOS	5.26×10^{-7}	88	[22]
	Co-TEOS	2.48×10^{-7}	50	[21]
	Mg-TEOS	7.00×10^{-8}	204	[22]
	Ni-TEOS	2.73×10^{-8}	160	[23]

Polymeric membranes	Poly(trimethylsilylpropyne)	5.41×10^{-6}	2	[24]
	Poly(tert-butyl acetylene)	3.85×10^{-7}	115	[25]
	Isotactic PMMA	4.32×10^{-10}	921	[26]
	Atactic PMMA	1.51×10^{-9}	385	[26]
	Syndiotactic PMMA	1.57×10^{-9}	362	[26]
	Poly[4-bis(trimethylsilyl-methyl styrene)]	1.61×10^{-7}	400	[24]
	Polybenzoxazinone imide (PBOI-2-Cu^{+})	1.24×10^{-9}	960	[27]
	Polyimide (1,1-6FDA-DIA)	1.05×10^{-8}	165	[28]
	Polyimide (NTDA-BAPHFDS(H))	1.74×10^{-8}	141	[29]
	Poly(amide-imide)	2.41×10^{-8}	103	[30]
	PIM-7	2.88×10^{-7}	21	[31]
	PIM-1	1.00×10^{-7}	14	[31]
	Poly(trimethylsilylpropyne-cophenylpropyne)	1.34×10^{-7}	3	[32]
	Poly(trimethylsilylpropyne)	6.70×10^{-8}	3	[32]
	PEI (Polyetherimide)	1.29×10^{-7}	2	[33]
	PF (Phenol formaldehyde)	1.71×10^{-8}	32	
	PPESKPoly-(phthalazinone ether sulfone ketone)	2.54×10^{-7}	39	
		3.95×10^{-8}	174	
		3.40×10^{-7}	73	
	TMSPPO (Trimethylsilyl-polyphenylene oxide)	6.17×10^{-7}	149	
	PR (Phenolic resin)	1.73×10^{-8}	29	
	PPO 15 PVP (Poly dimethyl phenylene oxide polyvinylpyrrolidone)	3.75×10^{-7}	165	
Zolite membranes	SAPO-34	1.75×10^{-7}	4	[34]
	Zeolite	2.00×10^{-8}	53	[34]
	Zeolite-β	4.00×10^{-7}	67	[35]
	H-MFI + CCD	2.50×10^{-8}	140	[36]
	AM-2	4.50×10^{-9}	45	[37]
	AM-2	4.40×10^{-8}	40	[38]
	MFI + CVD	3.96×10^{-7}	63	[39]
	LTA	5.00×10^{-7}	5	[40]
	LTA	3.00×10^{-7}	4	[41]
	FAU	4.00×10^{-7}	6	[42]
	LTA	8.10×10^{-7}	7	[43]
MOF membranes	ZIF-8/ TiO_2 disk	6.04×10^{-8}	12	[44]
	ZIF-8/ α-Al_2O_3 disk	2.35×10^{-7}	12	[45]
	ZIF-22/ APTES-modified TiO_2 disk	1.60×10^{-7}	6	[46]
	ZIF-90/ APTES-modified TiO_2 disk	2.48×10^{-7}	12	[47]
	ZIF-95/ APTES-modified α-Al_2O_3 disk	2.16×10^{-7}	10	[48]
	ZIF-8/ ZnO activated α-Al_2O_3 tubes	6.39×10^{-7}	8	[49]
	ZIF-8/ Organic ligand modified α-Al_2O_3 disk	1.73×10^{-7}	12	[46]
	ZIF-94	4.20×10^{-9}	136	[50]
	ZIF-8	3.40×10^{-8}	2	[51]
	ZIF-8	3.40×10^{-8}	7	[52]
	CUBTC	1.58×10^{-6}	4	[53]

	ZIF-8		2.01×10^{-5}	9	[54]
	CUBTC		2.01×10^{-6}	5	[55]
	ZIF-7		2.00×10^{-9}	35	[56]
Mixed-matrix membrane	6FDA–durene	ZIF-71	1.52×10^{-6}	7	[57]
	PIM-1	Fumed-silica	7.20×10^{-8}	4	[58]
	PIM-1	ZIF-8	1.94×10^{-6}	15	[59]
	PIM-1	Silicalite-1MFI	3.00×10^{-7}	11	[60]
	PDMS41	CNT	2.65×10^{-8}	4	[61]
	Pebaxs	GO	2.79×10^{-9}	8	[62]
	Polyether	diamine	4.65×10^{-9}	9	[63]
	PEO	Silica	7.42×10^{-8}	4	[64]
	PEG	Silica	2.83×10^{-8}	4	[65]
	PTMSP	Fumed silica	5.48×10^{-8}	3	[66]
	PTMSP	TiO_2	1.92×10^{-7}	3	[66]
	PTMSP	Trimethylsilylglucose	7.95×10^{-8}	11	[67]
	PMP	Fumed silica	4.78×10^{-8}	4	[68]
	PMP	TiO_2	1.86×10^{-7}	4	[68]
	Teflon	AF	1.19×10^{-6}	5	[69]

Table S3. Permeation data from different types of membranes for N_2/SF_6 separation reported in the reference

Membrane type	Membrane material	Temperature [°C]	N_2 permeance [mol m^{-2} s^{-1} Pa^{-1}]	$\frac{P_{N_2}}{P_{SF_6}}$ [-]	Ref.
Aminosilica membranes	BTPA	200	5.63×10^{-8}	67	This work
	BTPA	200	3.92×10^{-8}	45	
	BTPA	200	4.04×10^{-8}	31	
	Ag-BTPA	200	4.07×10^{-8}	14	
	Ag-BTPA	200	7.18×10^{-8}	17	
	Cu-BTPA	200	3.76×10^{-7}	131	
	Cu-BTPA	200	5.55×10^{-7}	90	
	Ni-BTPA	200	1.65×10^{-7}	1223	
	Ni-BTPA	200	3.75×10^{-7}	1900	
	Ni-BTPA	200	2.55×10^{-7}	1041	
Polymeric membranes	3-aminopropyl trimethoxysilane (APrTMOS)	-	9.98×10^{-9}	11	[70]
	Poly(1-trimethylsilyl-1-propyne)	0	2.58×10^{-6}	3.3	[71]
	Poly(1-trimethylsilyl-1-propyne)	0	2.81×10^{-7}	0.4	[71]
	Poly(4-methyl-1-pentene)	40	3.41×10^{-9}	194	[72]
	Poly(4-methyl-1-pentene)	40	3.45×10^{-9}	242	[72]
	Polydimethylsiloxane	25	1.07×10^{-7}	1	[73]
	Polyimide	-	1.00×10^{-7}	46	[74]
	Polyether block amide (PEBAX)	25	3.08×10^{-9}	3	[73]
	Polycarbonate (Standard-PC)	50	1.91×10^{-9}	2	[75]
	Polyethersulfone	25	5.06×10^{-9}	6	[76]

	Polyimide (Matrimid)	40	1.34×10^{-9}	66	[77]
	Polyimide (PA4050-P3)	25	3.35×10^{-10}	44	[78]
	Polyimide	25	3.62×10^{-8}	100	[79]
	Polyimide	25	3.68×10^{-10}	39	[80]
	Polyimide (PA4050-P3)	25	3.35×10^{-10}	44	[75]
	Polysulfone	25	1.61×10^{-9}	24	[78]
	Polysulfone	25	2.28×10^{-9}	19	[80]
	Polysulfone (MF/1008P)	25	1.61×10^{-9}	23.6	[75]
	Tetra-bromo polycarbonate	25	2.21×10^{-9}	2.5	[80]
	Polysulfone	45	2.96×10^{-9}	45	[75]
		35	2.51×10^{-9}	31	
		25	1.62×10^{-9}	24	
	Tetrabromopolycarbonate	45	2.74×10^{-9}	4	
		35	2.42×10^{-9}	3	
		25	2.18×10^{-9}	3	
	Polyimide	45	7.33×10^{-10}	78	
		35	4.72×10^{-10}	57	
		25	3.26×10^{-10}	44	
	Matrimid	25	8.37×10^{-10}	39	[77]
		50	1.21×10^{-9}	62	
		75	1.64×10^{-9}	92	
		100	2.11×10^{-9}	110	
		125	2.81×10^{-9}	115	
		150	3.55×10^{-9}	112	
		175	4.42×10^{-9}	104	
		200	5.26×10^{-9}	96	
	Poly(4-methyl-1-pentene)	30	2.53×10^{-9}	476	[72]
	Poly(4-methyl-1-pentene)	50	4.52×10^{-9}	165	
	Poly(4-methyl-1-pentene)	55	5.02×10^{-9}	95	
	Poly(4-methyl-1-pentene)	60	5.59×10^{-9}	67	
Silica membranes	TEOS/BTPA 400	200	3.20×10^{-8}	320	[81]
	TEOS/BTPA 500	200	5.54×10^{-9}	55	
	TEOS/BTPA 600	200	4.10×10^{-8}	2	
	PrTMOS	200	5.00×10^{-10}	110	[82]
	PrTMOS	300	7.00×10^{-9}	240	
	TMOS	200	1.00×10^{-11}	3	
	BTESE-acid	200	3.00×10^{-8}	333	[83]
	BTESE-swing	200	2.00×10^{-8}	200	
	BTESE-100°C	100	7.00×10^{-9}	4	[84]
	BTESE-200°C	100	7.00×10^{-8}	88	
	BTESE-300°C	100	9.00×10^{-8}	113	
Zeolite membranes	MFI-12h	25	1.40×10^{-6}	25	[85]
	MFI-6h	25	1.50×10^{-6}	75	
	MFI-3h	25	4.40×10^{-6}	40	
	MFI/S-1 (α- Al_2O_3)	25	1.40×10^{-6}	40	
	MFI/ZSM-5 (α- Al_2O_3)	25	2.94×10^{-6}	41	
	MFI/ZSM-5 (CTI-Al_2O_3-TiO_2)	25	2.50×10^{-6}	35	
	MFI/ZSM-5 (Al_2O_3-TiO_2)	25	2.50×10^{-6}	30	
	MFI/ZSM-5 (α- Al_2O_3)	25	3.70×10^{-6}	40	
	MFI/ZSM-5 (α- Al_2O_3)	25	5.20×10^{-6}	40	

	MFI/ZSM-5 (Inocermia-α-Al_2O_3)	25	3.80×10^{-6}	50	
	MFI/S-1 (Hyflux-α- Al_2O_3)	25	8.20×10^{-7}	40	
	MFI/S-1 (Hyflux-α- Al_2O_3)	25	7.60×10^{-7}	30	
	Chabazite 130 °C	130	1.00×10^{-8}	3	
	Chabazite 145 °C	130	1.60×10^{-8}	30	[86]
	Chabazite 160 °C	130	8.00×10^{-9}	20	

References

1. Yu, L., et al., *Fabrication and CO2 permeation properties of amine-silica membranes using a variety of amine types.* Journal of Membrane Science, 2017. **541**: p. 447-456.
2. De Lange, R., K. Keizer, and A. Burggraaf, *Analysis and theory of gas transport in microporous sol-gel derived ceramic membranes.* Journal of membrane science, 1995. **104**(1-2): p. 81-100.
3. Kanezashi, M., et al., *Gas permeation properties for organosilica membranes with different Si/C ratios and evaluation of microporous structures.* AIChE Journal, 2017. **63**(10): p. 4491-4498.
4. Lee, H.R., et al., *Evaluation and fabrication of pore-size-tuned silica membranes with tetraethoxydimethyl disiloxane for gas separation.* AIChE journal, 2011. **57**(10): p. 2755-2765.
5. Nagasawa, H., et al., *Modified gas-translation model for prediction of gas permeation through microporous organosilica membranes.* AIChE Journal, 2014. **60**(12): p. 4199-4210.
6. Guo, M., et al., *Fine-tuned, molecular-composite, organosilica membranes for highly efficient propylene/propane separation via suitable pore size.* AIChE Journal, 2020. **66**(4): p. e16850.
7. Xu, R., et al., *New insights into the microstructure-separation properties of organosilica membranes with ethane, ethylene, and acetylene bridges.* ACS applied materials & interfaces, 2014. **6**(12): p. 9357-9364.
8. Jabbari, A., et al., *Surface modification of α-alumina support in synthesis of silica membrane for hydrogen purification.* International journal of hydrogen energy, 2014. **39**(32): p. 18585-18591.
9. Igi, R., et al., *Characterization of Co-doped silica for improved hydrothermal stability and application to hydrogen separation membranes at high temperatures.* Journal of the American Ceramic Society, 2008. **91**(9): p. 2975-2981.
10. Darmawan, A., et al., *Binary iron cobalt oxide silica membrane for gas separation.* Journal of Membrane Science, 2015. **474**: p. 32-38.
11. Kanezashi, M., et al., *Organic–inorganic hybrid silica membranes with controlled silica network size: preparation and gas permeation characteristics.* Journal of Membrane Science, 2010. **348**(1-2): p. 310-318.
12. ten Hove, M., A. Nijmeijer, and L. Winnubst, *Facile synthesis of zirconia doped hybrid organic inorganic silica membranes.* Separation and purification technology, 2015. **147**: p. 372-378.
13. Yoshino, Y., et al., *Development of tubular substrates, silica based membranes and membrane modules for hydrogen separation at high temperature.* Journal of Membrane Science, 2005. **267**(1-2): p. 8-17.
14. Tsuru, T., et al., *Membrane reactor performance of steam reforming of methane using hydrogen-permselective catalytic SiO2 membranes.* Journal of Membrane Science, 2008. **316**(1-2): p. 53-62.
15. Kanezashi, M. and M. Asaeda, *Hydrogen permeation characteristics and stability of Ni-doped silica membranes in steam at high temperature.* Journal of Membrane Science, 2006. **271**(1-2): p. 86-93.
16. Suda, H., et al., *Preparation and gas permeation properties of silicon carbide-based inorganic membranes for hydrogen separation.* Desalination, 2006. **193**(1-3): p. 252-255.
17. Nomura, M., et al., *Preparation of a stable silica membrane by a counter diffusion chemical vapor deposition method.* Journal of membrane science, 2005. **251**(1-2): p. 151-158.
18. Choi, H.-S., C.-H. Ryu, and G.-J. Hwang, *Obtention of ZrO2–SiO2 hydrogen permselective membrane by chemical vapor deposition method.* Chemical engineering journal, 2013. **232**: p. 302-309.
19. Castricum, H.L., et al., *Tuning the nanopore structure and separation behavior of hybrid organosilica membranes.* Microporous and mesoporous materials, 2014. **185**: p. 224-234.
20. Song, H., Y. Wei, and H. Qi, *Tailoring pore structures to improve the permselectivity of organosilica membranes by tuning calcination parameters.* Journal of Materials Chemistry A, 2017. **5**(47): p. 24657-24666.
21. Liu, L., et al., *Influence of sol–gel conditioning on the cobalt phase and the hydrothermal stability of cobalt oxide silica membranes.* Journal of Membrane Science, 2015. **475**: p. 425-432.
22. Karakiliç, P., et al., *Sol-gel processed magnesium-doped silica membranes with improved H2/CO2 separation.* Journal of membrane science, 2017. **543**: p. 195-201.
23. Kanezashi, M. and M. Asaeda, *Stability of H2-permeselective Ni-doped silica membranes in steam at high temperature.* Journal of chemical engineering of Japan, 2005. **38**(11): p. 908-912.
24. Robeson, L.M., *Correlation of separation factor versus permeability for polymeric membranes.* Journal of membrane science, 1991. **62**(2): p. 165-185.
25. Takada, K., et al., *Gas permeability of polyacetylenes carrying substituents.* Journal of applied polymer science, 1985. **30**(4): p. 1605-1616.

26. Min, K. and D. Paul, *Effect of tacticity on permeation properties of poly (methyl methacrylate).* Journal of Polymer Science Part B: Polymer Physics, 1988. **26**(5): p. 1021-1033.
27. Polotskaya, G., et al., *Gas transport properties of polybenzoxazinoneimides and their prepolymers.* Polymer, 2005. **46**(11): p. 3730-3736.
28. Rezac, M.E. and B. Schöberl, *Transport and thermal properties of poly (ether imide)/acetylene-terminated monomer blends.* Journal of membrane science, 1999. **156**(2): p. 211-222.
29. Tanaka, K., et al., *Gas permeation and separation properties of sulfonated polyimide membranes.* Polymer, 2006. **47**(12): p. 4370-4377.
30. Fritsch, D. and N. Avella, *Synthesis and properties of highly gas permeable poly (amide-imide) s.* Macromolecular Chemistry and Physics, 1996. **197**(2): p. 701-714.
31. Budd, P.M., et al., *Gas separation membranes from polymers of intrinsic microporosity.* Journal of Membrane Science, 2005. **251**(1-2): p. 263-269.
32. Nagai, K., A. Higuchi, and T. Nakagawa, *Gas permeability and stability of poly (1-trimethylsilyl-1-propyne-co-1-phenyl-1-propyne) membranes.* Journal of Polymer Science Part B: Polymer Physics, 1995. **33**(2): p. 289-298.
33. Itta, A.K., H.-H. Tseng, and M.-Y. Wey, *Fabrication and characterization of PPO/PVP blend carbon molecular sieve membranes for H2/N2 and H2/CH4 separation.* Journal of Membrane Science, 2011. **372**(1-2): p. 387-395.
34. Yu, M., et al., *H2 separation using defect-free, inorganic composite membranes.* Journal of the American Chemical Society, 2011. **133**(6): p. 1748-1750.
35. Li, L., et al., *The preparation and gas separation properties of zeolite/carbon hybrid membranes.* Journal of Materials Science, 2015. **50**(6): p. 2561-2570.
36. Masuda, T., et al., *Modification of pore size of MFI-type zeolite by catalytic cracking of silane and application to preparation of H2-separating zeolite membrane.* Microporous and mesoporous materials, 2001. **48**(1-3): p. 239-245.
37. Kalyakin, A., et al., *Characterization of proton-conducting electrolyte based on La0. 9Sr0. 1YO3–δ and its application in a hydrogen amperometric sensor.* Sensors and Actuators B: Chemical, 2016. **225**: p. 446-452.
38. Pakhare, D., et al., *Characterization and activity study of the Rh-substituted pyrochlores for CO 2 (dry) reforming of CH 4.* Applied Petrochemical Research, 2013. **3**(3-4): p. 117-129.
39. Tang, Z., J. Dong, and T.M. Nenoff, *Internal surface modification of MFI-type zeolite membranes for high selectivity and high flux for hydrogen.* Langmuir, 2009. **25**(9): p. 4848-4852.
40. Brandão, A., et al., *Enhanced low-temperature proton conduction in Sr0. 02La0. 98NbO4− δ by scheelite phase retention.* Chemistry of Materials, 2010. **22**(24): p. 6673-6683.
41. Shimura, T., S. Fujimoto, and H. Iwahara, *Proton conduction in non-perovskite-type oxides at elevated temperatures.* Solid State Ionics, 2001. **143**(1): p. 117-123.
42. Brandao, A., et al., *B-site substitutions in LaNb1− xMxO4− δ materials in the search for potential proton conductors (M= Ga, Ge, Si, B, Ti, Zr, P, Al).* Journal of Solid State Chemistry, 2011. **184**(4): p. 863-870.
43. Haugsrud, R., *Defects and transport properties in Ln6WO12 (Ln= La, Nd, Gd, Er).* Solid State Ionics, 2007. **178**(7-10): p. 555-560.
44. Kwon, H.T. and H.-K. Jeong, *In situ synthesis of thin zeolitic–imidazolate framework ZIF-8 membranes exhibiting exceptionally high propylene/propane separation.* Journal of the American Chemical Society, 2013. **135**(29): p. 10763-10768.
45. Bux, H., et al., *Zeolitic imidazolate framework membrane with molecular sieving properties by microwave-assisted solvothermal synthesis.* Journal of the American Chemical Society, 2009. **131**(44): p. 16000-16001.
46. Huang, A., et al., *Molecular-sieve membrane with hydrogen permselectivity: ZIF-22 in LTA topology prepared with 3-aminopropyltriethoxysilane as covalent linker.* Angewandte Chemie, 2010. **122**(29): p. 5078-5081.
47. Huang, A., W. Dou, and J.r. Caro, *Steam-stable zeolitic imidazolate framework ZIF-90 membrane with hydrogen selectivity through covalent functionalization.* Journal of the American Chemical Society, 2010. **132**(44): p. 15562-15564.
48. Xie, Z., et al., *Deposition of chemically modified α-Al 2 O 3 particles for high performance ZIF-8 membrane on a macroporous tube.* Chemical communications, 2012. **48**(48): p. 5977-5979.
49. Yao, J., et al., *Contra-diffusion synthesis of ZIF-8 films on a polymer substrate.* Chemical Communications, 2011. **47**(9): p. 2559-2561.
50. Cacho-Bailo, F., et al., *Sequential amine functionalization inducing structural transition in an aldehyde-containing zeolitic imidazolate framework: application to gas separation membranes.* CrystEngComm, 2017. **19**(11): p. 1545-1554.
51. Liu, Y., et al., *In situ synthesis of MOF membranes on ZnAl-CO3 LDH buffer layer-modified substrates.* Journal of the American Chemical Society, 2014. **136**(41): p. 14353-14356.
52. Hu, Y., et al., *Zeolitic imidazolate framework/graphene oxide hybrid nanosheets as seeds for the growth of ultrathin molecular sieving membranes.* Angewandte Chemie, 2016. **128**(6): p. 2088-2092.
53. Mao, Y., et al., *Room temperature synthesis of free-standing HKUST-1 membranes from copper hydroxide nanostrands for gas separation.* Chemical Communications, 2013. **49**(50): p. 5666-5668.
54. Hou, J., et al., *Formation of ultrathin, continuous metal–organic framework membranes on flexible polymer substrates.* Angewandte Chemie International Edition, 2016. **55**(12): p. 3947-3951.
55. Mao, Y., et al., *Pressure-assisted synthesis of HKUST-1 thin film on polymer hollow fiber at room temperature toward gas separation.* ACS applied materials & interfaces, 2014. **6**(6): p. 4473-4479.
56. Cacho-Bailo, F., et al., *Metal-organic framework membranes on the inner-side of a polymeric hollow fiber by microfluidic synthesis.* Journal of Membrane Science, 2015. **476**: p. 277-285.
57. Japip, S., et al., *Highly permeable zeolitic imidazolate framework (ZIF)-71 nano-particles enhanced polyimide membranes for gas separation.* Journal of Membrane Science, 2014. **467**: p. 162-174.

58. Ahn, J., et al., *Gas transport behavior of mixed-matrix membranes composed of silica nanoparticles in a polymer of intrinsic microporosity (PIM-1).* Journal of membrane science, 2010. **346**(2): p. 280-287.
59. Bushell, A.F., et al., *Gas permeation parameters of mixed matrix membranes based on the polymer of intrinsic microporosity PIM-1 and the zeolitic imidazolate framework ZIF-8.* Journal of Membrane Science, 2013. **427**: p. 48-62.
60. Mason, C.R., et al., *New organophilic mixed matrix membranes derived from a polymer of intrinsic microporosity and silicalite-1.* Polymer, 2013. **54**(9): p. 2222-2230.
61. Kim, S., T.W. Pechar, and E. Marand, *Poly (imide siloxane) and carbon nanotube mixed matrix membranes for gas separation.* Desalination, 2006. **192**(1-3): p. 330-339.
62. Shen, J., et al., *Membranes with fast and selective gas-transport channels of laminar graphene oxide for efficient CO2 capture.* Angewandte Chemie, 2015. **127**(2): p. 588-592.
63. Sforca, M., I. Yoshida, and S. Nunes, *Organic–inorganic membranes prepared from polyether diamine and epoxy silane.* Journal of membrane science, 1999. **159**(1-2): p. 197-207.
64. Xia, J., S. Liu, and T.-S. Chung, *Effect of end groups and grafting on the CO2 separation performance of poly (ethylene glycol) based membranes.* Macromolecules, 2011. **44**(19): p. 7727-7736.
65. Xia, J., et al., *Liquidlike poly (ethylene glycol) supported in the organic–inorganic matrix for CO2 removal.* Macromolecules, 2011. **44**(13): p. 5268-5280.
66. Shao, L., J. Samseth, and M.B. Hägg, *Crosslinking and stabilization of nanoparticle filled poly (1-trimethylsilyl-1-propyne) nanocomposite membranes for gas separations.* Journal of applied polymer science, 2009. **113**(5): p. 3078-3088.
67. Qiu, J., J.-M. Zheng, and K.-V. Peinemann, *Gas transport properties in a novel poly (trimethylsilylpropyne) composite membrane with nanosized organic filler trimethylsilylglucose.* Macromolecules, 2006. **39**(12): p. 4093-4100.
68. Shao, L., J. Samseth, and M.-B. Hägg, *Crosslinking and stabilization of nanoparticle filled PMP nanocomposite membranes for gas separations.* Journal of Membrane Science, 2009. **326**(2): p. 285-292.
69. Golemme, G., et al., *Surface modification of molecular sieve fillers for mixed matrix membranes.* Colloids and Surfaces A: Physicochemical and Engineering Aspects, 2018. **538**: p. 333-342.
70. Ishii, K., et al., *Development of silica membranes to improve dehydration reactions.* Journal of the Japan Petroleum Institute, 2019. **62**(5): p. 211-219.
71. Srinivasan, R., S. Auvil, and P. Burban, *Elucidating the mechanism (s) of gas transport in poly [1-(trimethylsilyl)-1-propyne](PTMSP) membranes.* Journal of Membrane Science, 1994. **86**(1-2): p. 67-86.
72. Wolińska-Grabczyk, A., et al., *Separation of SF6 from binary mixtures with N2 using commercial poly (4-methyl-1-pentene) films.* Separation Science and Technology, 2011. **46**(8): p. 1231-1240.
73. Kim, H., et al., *Permeation properties of single gases ($ N_2 $, $ O_2 $, $ SF_6 $, $ CF_4 $) through PDMS and PEBAX membranes.* Membrane journal, 2012. **22**(3): p. 201-207.
74. Zhu, G., et al., *Molecularly mixed composite membranes for advanced separation processes.* Angewandte Chemie International Edition, 2019. **58**(9): p. 2638-2643.
75. Lee, S., et al., *Separation of sulfur hexafluoride (SF6) from ternary gas mixtures using commercial polysulfone (PSf) hollow fiber membranes.* Journal of membrane science, 2014. **452**: p. 311-318.
76. Kim, D.-H., et al., *Separation of N 2/SF 6 binary mixtures using polyethersulfone (PESf) hollow fiber membrane.* Korean Journal of Chemical Engineering, 2012. **29**(8): p. 1081-1085.
77. Dai, Y., et al., *Fabrication of defect-free Matrimid® asymmetric membranes and the elevated temperature application for N2/SF6 separation.* Journal of Membrane Science, 2019. **577**: p. 258-265.
78. Choi, J.-W., et al., *Separation of sulfur hexafluoride from a nitrogen/sulfur hexafluoride mixture using a polymer hollow fiber membrane.* Water, Air, & Soil Pollution, 2014. **225**(2): p. 1807.
79. Yamamoto, O., T. Takuma, and M. Kinouchi, *Recovery of SF/sub 6/from N/sub 2//SF/sub 6/gas mixtures by using a polymer membrane.* IEEE Electrical Insulation Magazine, 2002. **18**(3): p. 32-37.
80. Ko, Y.-d., H.-K. Lee, and S.-U. Hong, *Separation of $ SF_6 $ from $ SF_6/N_2 $ Mixtures Using Polymeric Membranes.* Membrane Journal, 2012. **22**(1): p. 72-76.
81. Hong, Q., *Preparation of composite microporous silica membranes using TEOS and 1, 2-bis (triethoxysilyl) ethane as precursors for gas separation.* Chinese Journal of Chemical Engineering, 2011. **19**(3): p. 404-409.
82. Nomura, M., et al., *Preparation of silica hybrid membranes for high temperature gas separation.* Desalination and Water Treatment, 2010. **17**(1-3): p. 288-293.
83. Yu, X., et al., *Network engineering of a BTESE membrane for improved gas performance via a novel pH-swing method.* Journal of Membrane Science, 2016. **511**: p. 219-227.
84. Wang, J., et al., *Effect of calcination temperature on the PV dehydration performance of alcohol aqueous solutions through BTESE-derived silica membranes.* Journal of membrane science, 2012. **415**: p. 810-815.
85. Drobek, M., et al., *Coupling microwave-assisted and classical heating methods for scaling-up MFI zeolite membrane synthesis.* Journal of membrane science, 2012. **401**: p. 144-151.
86. Nouri, A., et al., *Potential separation of SF6 from air using chabazite zeolite membranes.* Chemical Engineering & Technology, 2014. **37**(2): p. 317-324.